Criteria Governing Electron Plasma Waves in a Two-Temperature Plasma

M. P. Dell, I. M. A. Gledhill, and M. A. Hellberg
Plasma Physics Research Institute, University of Natal, Durban, South Africa

Z. Naturforsch. **42 a**, 1175–1180 (1987); received June 15, 1987

Dedicated to Professor Dieter Pfirsch on his 60th Birthday

Using a technique based on the saddle-points of the dielectric function, criteria are found which govern the behaviour of electron plasma waves in plasmas with two electron populations having different temperatures.

1. Introduction

Plasmas with two electron populations having different temperatures are known to occur in thermonuclear fusion research devices, laser plasma experiments, space plasmas, multipole laboratory devices, etc. A number of studies in small basic research machines [1, 2, 3] have shown that in such plasmas, two electron plasma wave (EPW) modes may under certain circumstances occur simultaneously. One of the modes was found to propagate at frequencies below the plasma frequency, ω_p, unlike the principal EPW mode predicted by fluid theory, which has

$$\omega^2 = \omega_p^2 + \tfrac{3}{2} k^2 C_e^2 , \tag{1}$$

where $C_e = (2\,T_e/m_e)^{1/2}$ is the electron thermal speed.

It is well known that kinetic theory [4] predicts the existence in a simple plasma of an infinite number of higher order modes (HOM) in addition to the principal or Landau mode. These HOM are more heavily-damped and may have frequencies both above and below ω_p. They have been studied in detail by Derfler and Simonen [5].

The observation of two EPW modes in a two-temperature plasma has been explained by the coupling of the principal and a higher order mode in such a plasma [6]. However, no general criteria have been given to enable one to distinguish the conditions under which two modes may occur.

The Vlasov-based dispersion relation for EPW in a two-temperature plasma exhibits certain similarities to that for ion acoustic waves (IAW) in a two-ion plasma. In the latter case, as the fraction of lighter ions is increased from 0 to 1, two types of wave behaviour may occur [7]. Depending on the values of the plasma parameters, either the principal mode of the heavy ion plasma undergoes a continuous change of phase velocity and becomes identified with the principal light ion mode (PLM), or it becomes increasingly heavily damped, whilst one of the HOM loses its damping and is transformed into the PLM. In that case there is a range of values of light ion fraction for which both modes may be observed.

The criteria governing these two types of behaviour of IAW in a two-ion plasma have been discussed in detail in a recent paper by Gledhill and Hellberg [8], which we shall henceforth refer to as Paper I. They have shown that the distinguishing criterion may be derived by considering the saddle points of the dielectric function.

In this paper we apply the technique used in I to the case of EPW in a two-temperature plasma, and hence obtain criteria for the possible simultaneous occurrence of two EPW modes. Preliminary results were presented earlier [9]. In § 2 we outline the theory and the technique for the case of real k and complex ω, while in § 3 the case of complex k is dealt with. In § 4 the results are related to some experimental studies.

2. Complex ω

The dispersion relation for plane, linear electron plasma waves with real k and complex ω in an infinite, homogeneous, field-free collisionless plasma with two populations of Maxwellian electrons having different temperatures may be written

0932-0784 / 87 / 1000-1175 $ 01.30/0. – Please order a reprint rather than making your own copy.

in the form

$$\varepsilon = 1 - \frac{1}{2k^2\lambda_{D_c}^2}\frac{n_c}{n_i}Z'(\omega/kC_c) - \frac{1}{2k^2\lambda_{Dh}^2}\frac{n_h}{n_i}Z'(\omega/kC_h) = 0\,. \quad (2)$$

Here the subscripts c and h refer to the cold and hot electron components, respectively, C is a thermal speed, λ_D a Debye length based on the ion density n_i, and $Z'(z)$ the derivative of $Z(z)$, the usual plasma dispersion function tabulated by Fried and Conte [10]. As usual, the ion contribution has been ignored for the high-frequency EPW.

Introducing the parameters $\lambda_D = (\varepsilon_0 T_c/n_i e^2)^{1/2}$, the Debye length for the cold component, $\beta = T_h/T_c$, the ratio of hot to cold electron temperature, and $F = n_h/n_i$, the fraction of electrons which are hot, we may write this as

$$G(u) = \left(\frac{F}{\beta}\right)Z'(u/\sqrt{\beta}) + (1-F)Z'(u) = 2k^2\lambda_D^2\,. \quad (3)$$

The complex function $G(u)$ has real and imaginary parts G_r and G_i, respectively, and its argument u is the complex phase velocity normalized to the thermal velocity of the cold electron component,

$$u = \left(\frac{\omega}{k}\right)\Big/\left\{\frac{2T_c}{m_e}\right\}^{1/2}.$$

This equation may be compared with the dispersion relation for IAW in a two-ion plasma, as written in (9) of Paper I, viz.

$$G(\mu) = fZ'(\mu/\sqrt{M}) + (1-f)Z'(\mu) = \zeta = 2(1+k^2\lambda_D^2)/\theta\,. \quad (4)$$

Here the number density fraction of lighter ions is given by $f = n_l/n_e$, the mass ratio of the two ion species is $M = m_h/m_l$, the electron-ion temperature ratio is $\theta = T_e/T_i$ and $\mu = \omega/kC_h$ is the complex phase velocity normalized to the heavy ion thermal velocity.

It is seen that for $F \ll 1$, (3) and (4) are similar if we make the substitutions

$$\beta = M\,, \quad F = \beta f\,, \quad 2k^2\lambda_D^2 = \zeta\,. \quad (5)$$

Clearly the results of Paper I may thus be adapted to the present case. However, for clarity we shall outline the technique used.

As the right hand side of (3) is real, all solutions must lie on the contours $G_i = 0$ in complex velocity space, while solutions for specific k will occur at the intersections of these contours with the contours $G_r = 2k^2\lambda_D^2$. Contours of both G_r and G_i intersect at the saddle points of G. For particular critical values of F, named F_j^*, saddle points in G_i occur at positions S_j, such that $G_i(S_j) = 0$. Thus when $F = F_j^*$, two roots approach each other in the complex u plane and pass through S_j as $k\lambda_D$ is varied (Figure 1). The value of $k\lambda_D$ at which the roots coincide at the saddle point S_j is the critical value $k_j^*\lambda_D$. As $k\lambda_D$ is increased through $k_j^*\lambda_D$ for a given value of F, the two roots pass anti-clockwise around this saddle point for $F < F_j^*$ and clockwise for $F > F_j^*$. It may also be demonstrated that the paths traced by the roots as F is varied reconnect similarly as $k\lambda_D$ passes through its critical value $k^*\lambda_D$.

The function $G(u)$ has an infinite number of saddle points arising from those in $Z'(u)$ (subscripts $j = 0, 1, 2, \ldots$), and at least one produced by the addition of the terms which form the function $G(u)$ (subscript β). Thus this saddle point does not occur for $F = 0$ or $F = 1$, but only for intermediate values. As is the case for the analogous saddle point S_M in Paper I, the position of the saddle point S_β is strongly dependent on β.

Critical values of $k_j^*\lambda_D$ and F_j^*, calculated using the iterative method described in Paper I, are plotted in Figs. 2 and 3. The behaviour of roots as F (or $k\lambda_D$) is varied is determined by the parameters β and $k\lambda_D$ (or F). Within each region delineated by the critical curves root behaviour remains qualitatively similar. If a critical curve is crossed, the

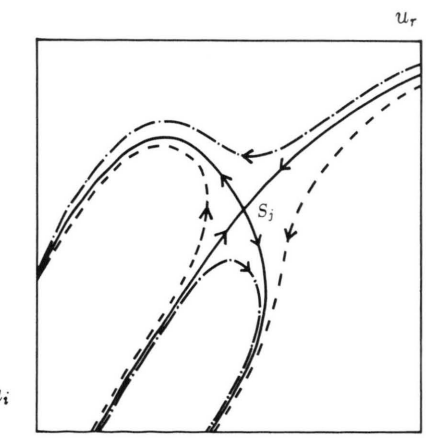

Fig. 1. Influence of saddle point S_j on paths traced by roots in the complex u plane as $k\lambda_D$ is increased. Root paths are shown for three values of F: $-\cdot-\cdot-$ $F < F_j^*$; —— $F = F_j^*$; – – – $F > F_j^*$.

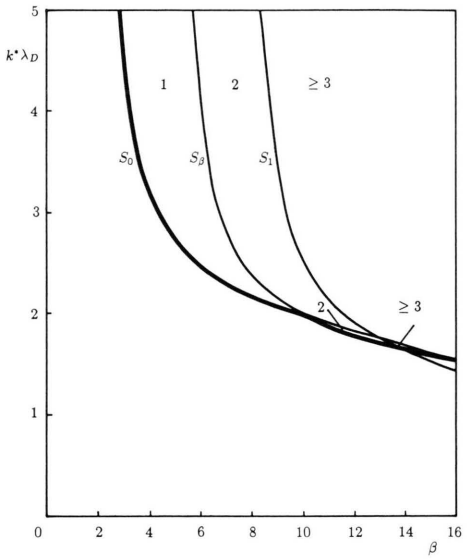

Fig. 2. Complex ω: Critical values of $k\lambda_D$ for the three most prominent saddle points. These govern continuity of modes as F is changed. The integers designate the higher order mode which couples with the principal mode.

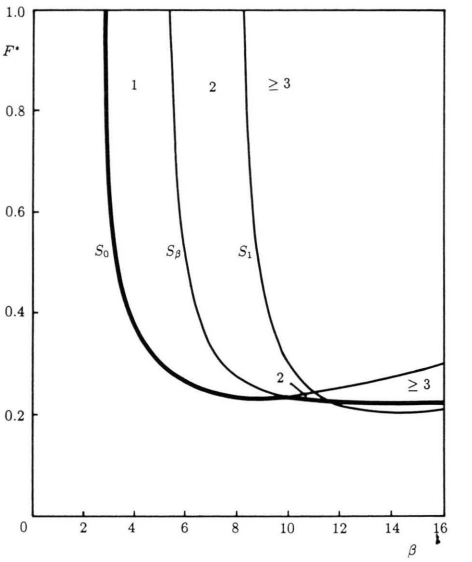

Fig. 3. Complex ω: Critical values of F for the three most prominent saddle points. These govern continuity of modes as $k\lambda_D$ is changed. The integers indicate which higher order mode couples with the principal mode.

topology of the root paths in the complex u plane changes. By investigating mode behaviour in the different regions, it is found that the curves indicated by bold lines divide regions in which the principal mode transforms continuously from those in which it becomes a HOM.

Thus suppose that in a plasma with a given β, the value of $k\lambda_D$ lies below the bold line in Figure 2. Then, as F, the fraction of electrons at the higher temperature, is increased from 0 to 1, the principal electron plasma wave associated with a plasma having all its electrons at the lower temperature – the principal cold mode (PCM) – will go over continuously into the principal hot electron mode (PHM), and thus only a single mode will be observed at all values of F. For values of $k\lambda_D$ lying above the critical curve, it is found that the PCM becomes increasingly damped as the fraction of hot electrons is increased. At the same time a higher order mode, which is strongly damped for $F=0$, exhibits reduced damping, and develops into the PHM. Over a range of intermediate values of F, it is possibe for two weakly-damped modes, having different phase velocities, to coexist. The integer marked in each region above the bold line indicates which higher order mode develops into the PHM.

When, instead, we choose a value of F and allow $k\lambda_D$ to increase from 0, then the root behaviour depends on the value of F relative to the F^* values plotted in Figure 3. The bold line plays a similar role to that outlined above, as do the integers marked in the different regions.

These two figures are in principle similar to Figs. 7 (allowing for the inverse relationship between $k\lambda_D$ and θ) and 8 of Paper I. Indeed it should be noted that one may obtain the critical values presented here from those found in Paper I by making the transformations

$$F^*(\beta) = \beta f^*/(1+(\beta-1)f^*)\,,$$

$$k^*\lambda_D(\beta) = \left\{\frac{\zeta^*/2}{1+(\beta-1)f^*}\right\}^{1/2}, \tag{6}$$

where in each case the critical values f^* and ζ^* are to be evaluated at a value of $M=\beta$.

3. Complex k

In many laboratory experiments a wave is driven at a real frequency ω and the spatial propagation and damping are observed. For such cases it is desirable to consider the case of complex k.

The dispersion relation may then be cast in the form

$$\left(\frac{F}{\beta}\right) Z'(u/\sqrt{\beta}) + (1-F)\,Z'(u) = (\omega^2/\omega_p^2)/u^2\,. \tag{7}$$

Here ω_p is the plasma frequency of the combined electron population. The calculation of critical F and ω/ω_p curves is facilitated if the right hand side is real, and thus we rewrite the equation as

$$H(u) = u^2\left[\left(\frac{F}{\beta}\right) Z'(u/\sqrt{\beta}) + (1-F)\, Z'(u)\right] = \omega^2/\omega_p^2 . \quad (8)$$

The complex function $H(u)$ has a similar set of saddle points S_β, S_0, S_1, S_2, ... to those of $G(u)$, although their positions are obviously modified slightly by the factor u^2.

Criteria governing the behaviour of the modes as the driving frequency ω, or rather the ratio ω/ω_p is varied, are illustrated in Figure 4. This shows the value of F^* at several saddle points in the dispersion function $H(u)$, plotted against the temperature ratio β. The behaviour of the principal mode as ω/ω_p is increased from 1 depends on the values of the parameters β and F relative to these critical curves. The principal mode is found to remain the least damped mode only if the point (β, F) lies below the curve corresponding to the saddle point S_β. If the point (β, F) lies in a region denoted by l, the principal mode behaves like the lth HOM when the frequency is much larger than ω_p.

It can be shown that for $\beta > 4$, the position of S_β when $F = F^*$ varies as

$$S_\beta \sim (1.5 - 0.4\,i)\sqrt{\beta} . \quad (9)$$

This may be compared with the finding in Paper I that the equivalent saddle point S_M in the ion acoustic case satisfies

$$S_M \sim (1.0 - 0.4\,i)\sqrt{M} \quad \text{for} \quad M > 10 .$$

If the fraction of hot electrons, F, is varied, the behaviour of the modes depends on the value of the normalized frequency ω/ω_p relative to the critical curves shown in Figure 5. The bold curve corresponding to the saddle point S_β marks the upper limit of ω/ω_p for which the principal mode of the cool electron component (PCM) develops continuously into the principal mode of the hot component (PHM), as F is increased from 0 to 1. Clearly, for $F = 0$ or 1, the least damped mode is just the appropriate Bohm-Gross mode, which propagates only for $\omega > \omega_p$, and hence the PCM can only develop into the PHM for $\omega > \omega_p$. Thus this case of continuous change between the principal modes (i.e. the case for which only a single mode would be observable for all values of F) is restricted to lie between the bold curve formed by S_β and the bold line at $\omega = \omega_p$.

For the region excluded in the above discussion, different HOM may become the least damped mode for high F and it is possible for two EPW modes to be observed for some values of F. The integers in Figure 5 indicate which HOM becomes the least

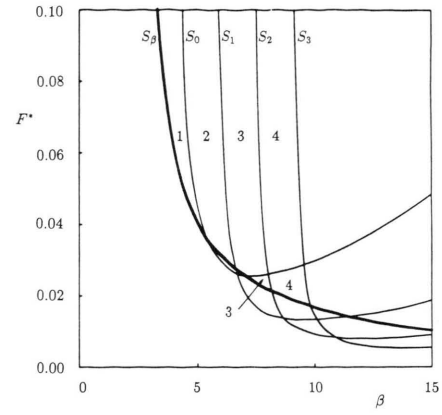

Fig. 4. Complex k: Critical values of F. If F lies below the bold line, the mode which is least damped when $\omega \sim \omega_p$ remains weakly damped as ω is increased. Otherwise, it develops into a higher order mode (indicated by the relevant integer) when $\omega \gg \omega_p$.

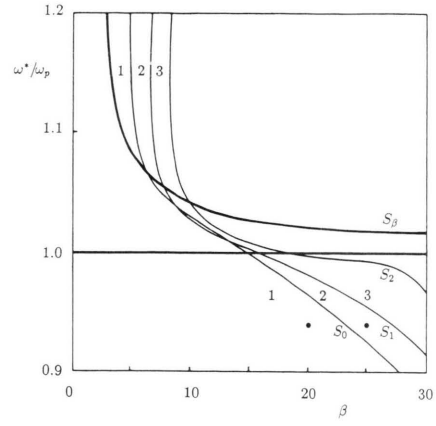

Fig. 5. Complex k: Critical values of ω/ω_p as a function of β. The integers indicate which higher order mode develops into the least damped mode as F is increased. For parameter combinations between the two bold lines, the PCM remains the least damped mode for all values of F. The solid circles indicate the parameter values used in Figure 6.

For the region excluded in the above discussion, different HOM may become the least damped mode for high F and it is possible for two EPW modes to be observed for some values of F. The integers in Figure 5 indicate which HOM becomes the least

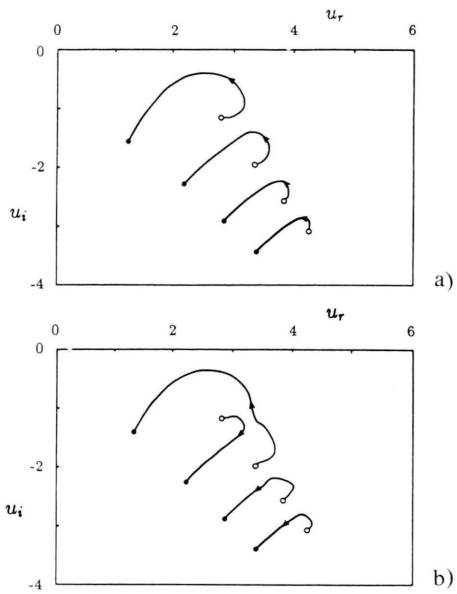

Fig. 6. Examples of the mode behaviour as F is varied, when $\omega < \omega_p$. Arrows show direction of increasing F. In each case $\omega/\omega_p = 0.94$; ○ $F = 0.0$; ● $F = 0.9$. In Fig. 6 (a), $\beta = 20$; in Figure 6 (b), $\beta = 25$.

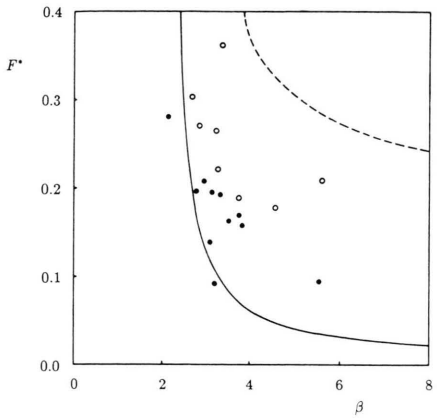

Fig. 7. Comparison of the experimental results of Ikezawa and Nakamura (1981) with the predictions of the saddle point method. Circles show conditions under which one (●) mode or two (○) modes are observed as ω/ω_p is varied. The theoretical boundary curves are calculated using the saddle point method for —— real ω and complex k; – – – real k and complex ω. The theoretical boundary curve of Ikezawa and Nakamura (1981) coincides with the solid curve shown here.

damped mode as F is increased. For $\omega/\omega_p > 1$, this least damped mode is the PHM, but for lower frequencies it is the first HOM. This is illustrated in Figures 6 (a) and (b), which show the root behaviour for two different values of β when $\omega < \omega_p$. The parameter values used are those marked in Figure 5. When $\beta = 20$, the first HOM remains the least damped mode as F is increased, while for $\beta = 25$, it is the second HOM which at large F has a lower damping rate (u_i smaller negative value), and thus dominates.

Finally, it will have been noted that these curves are in principle similar to those of Figs. 2 and 3. There is, however, an interesting difference. Whereas in the earlier case, the critical curve relating to continuity of modes depends on both the $j = 0$ and the $j = \beta$ curve, the only saddle point to play a significant role in the real ω case is S_β, i.e. that which arises from a combination of the two Z' functions in $G(u)$.

4. Comparison with Experiment

Much of what we have discussed is of theoretical interest, e.g. the importance of the saddle-point behaviour and the specification of the higher order mode which may play a role in a given situation. Nevertheless, there are aspects which are subject to experimental check.

Ikezawa and Nakamura [3] have observed electron plasma waves in a plasma with two Maxwellian electron components. For various combinations of the parameters β and F, dispersion measurements were taken over a range of ω/ω_p from 0.1 to 2.0. The plasma conditions under which two modes were obseved are shown as open circles in Figure 7. The closed circles indicate cases where only one mode was seen.

It might be expected that the theory outlined above should be able to differentiate between the two cases. The bold curve in Fig. 7 is the criterion from our analysis based on saddle points in the dispersion function for real ω and complex k, and overlaps the boundary which Ikezawa and Nakamura derived by inspecting solutions of the dispersion relation. When F lies below this curve, a single weakly damped principal mode should be continuously observable, while for larger values of F, two weakly damped modes should propagate. The corresponding criterion for complex ω and real k is included as a dashed curve for comparison.

Although the experimental data and the theoretical curve show similar trends and orders of

magnitude, quantitative agreement is lacking. Clearly there are many cases where one observes only one mode where two might be expected. It has been suggested [3] that the discrepancy arises from the fact that the observability of a wave depends not only on the damping, but also on the excitation coefficient. Thus if two weakly damped modes may propagate, only one will be observed if the two modes have substantially different excitation coefficients. However, as F is increased, the two weakly damped modes will propagate in more distinct ranges of ω/ω_p, and thus be observable separately as ω/ω_p is varied.

5. Effect of Collisions

For an electron-neutral collision frequency $\nu \ll \omega_p$, one may include collisional effects by replacing ω with $\omega + i\nu$ in the dispersion relation which becomes

$$G(u) = u^2 \{FZ'(u/\sqrt{\beta})/\beta + (1-F)Z'(u)\} = (\omega + i\nu)^2/\omega_p^2 . \quad (10)$$

Although the left-hand side does not depend explicitly on ν, collisions nevertheless affect the positions of the saddle points of $G(u)$, as the value of F in $G(u)$ has to satisfy (10).

The main observable effect of collisions is a reduction of the value of F^*, i.e. one finds that when collisions are included, the critical F curves of Fig. 4 are all lowered. Thus the switch from a one-mode to a two-mode situation occurs for a smaller fraction of light ions than is the case for the collision-free plasma. This is not altogether surprising, as like collisions, the introduction of light ions (small F) has a damping effect.

Collisions do, however, have a further effect, viz. the introduction of a further saddle point, which, because of its occurrence for non-zero ν only, we designate as S_ν. Like S_β, it arises from the superposition of the two surfaces related to the two terms in (10), and thus does not exist in a single-ion plasma. It appears not to play a role in the question of the one-mode or two-mode behaviour of the electron plasma wave.

We have seen that for the principal mode, (1), the real part of k, k_r, tends to zero as ω tends to ω_p. On the other hand collisions cause damping, i.e. a finite value of k_i. Thus for ω close to ω_p the principal mode has a relatively large normalized damping rate k_i/k_r, and it tends to behave like a higher order mode. Calculations for $F = 0.01$ and $\beta = 5$ showed that as ν is increased, the principal mode interacts with different higher order modes, the saddle point S_ν marking the position at which the interaction switches from one higher order mode to another.

6. Conclusion

In this paper we have used a numerical-geometric technique to consider the criteria governing the behaviour of electron plasma waves in a two-ion plasma. It involves a study of the saddle points of the dispersion function and their coincidence with roots of the dispersion relation. This technique was earlier applied to ion acoustic waves in a two-ion plasma [8]. We have now explored the criteria governing the possible occurrence of two EPW modes, both for complex ω and for complex k, as well as the effects of collisions.

Acknowledgements

This work was supported in part by the Foundation for Research Development of the CSIR.

[1] D. Henry and J. P. Treguier, J. Plasma Phys. **8,** 311 (1972).
[2] Y. Kawai, Y. Nakamura, T. Itoh, T. Hara, and T. Kawabe, J. Phys. Soc. Japan **38,** 876 (1975)
[3] S. Ikezawa and Y. Nakamura, J. Phys. Soc. Japan **50,** 962 (1981).
[4] L. Landau, J. Phys. **10,** 25 (1946).
[5] H. Derfler and T. C. Simonen, Phys. Fluids **12,** 269 (1969).
[6] S. Ikezawa and Y. Nakamura, J. Phys. Soc. Japan **46,** 1677 (1979).
[7] B. D. Fried, R. B. White, and T. J. Samec, Phys. Fluids **14,** 2388 (1971); Y. Nakamura, M. Nakamura, and T. Itoh, Univ. Tokyo ISAS RN 13 (1976); M. Nakamura, M. Ito, Y. Nakamura, and T. Itoh, Phys. Fluids **18,** 651 (1975); M. W. Tran and S. Coquerand, Helv. Phys. Acta **48,** 477 (1975).
[8] I. M. A. Gledhill and M. A. Hellberg, J. Plasma Phys. **36,** 75 (1986).
[9] I. M. A. Gledhill, M. P. Dell, and M. A. Hellberg, Proc. XVI Int. Conf. Phen. Ionized Gases, Düsseldorf 1983, p. 650.
[10] B. D. Fried and S. D. Conte, The Plasma Dispersion Function, Academic Press, New York 1961.